Synchronization and chaotic dynamics of coupled mechanical metronomes

Cite as: Chaos **19**, 043120 (2009); https://doi.org/10.1063/1.3266924
Submitted: 17 August 2009 • Accepted: 28 October 2009 • Published Online: 03 December 2009

Henning Ulrichs, Andreas Mann and Ulrich Parlitz

Synchronization and chaotic dynamics of coupled mechanical metronomes

Henning Ulrichs,[1,a)] Andreas Mann,[1] and Ulrich Parlitz[2]
[1]*I. Physikalisches Institut, University of Göttingen, D-37077 Göttingen, Friedrich-Hund-Platz 1, Göttingen, Germany*
[2]*III. Physikalisches Institut, University of Göttingen, D-37077 Göttingen, Friedrich-Hund-Platz 1, Göttingen, Germany*

(Received 17 August 2009; accepted 28 October 2009; published online 3 December 2009)

Synchronization scenarios of coupled mechanical metronomes are studied by means of numerical simulations showing the onset of synchronization for two, three, and 100 globally coupled metronomes in terms of Arnol'd tongues in parameter space and a Kuramoto transition as a function of coupling strength. Furthermore, we study the dynamics of metronomes where overturning is possible. In this case hyperchaotic dynamics associated with some diffusion process in configuration space is observed, indicating the potential complexity of metronome dynamics. © *2009 American Institute of Physics*. [doi:10.1063/1.3266924]

Metronomes are often viewed as paradigm of strictly periodic motion. Physically a metronome is a nonlinear self-sustained oscillator whose natural frequency is precisely tuned for practical applications, for example, to provide exact timing for musical exercises. Since the state space of a single metronome is two-dimensional, asymptotically only periodic oscillations or steady states may occur. This situation changes qualitatively if two or more metronomes are coupled and higher dimensional (chaotic) attractors are possible. Furthermore, coupled metronomes may exhibit synchronization phenomena reminiscent of Huygens' famous pendulum clocks. If two metronomes are coupled they exhibit typical phase-locking phenomena if their individual (uncoupled) frequencies almost coincide or are rationally related. For large ensembles of metronomes a collective transition to synchronization occurs in terms of a so-called Kuramoto transition. And, last but not least, it turns out that coupled metronomes may exhibit high-dimensional chaotic dynamics, in particular if overturnings are possible. These findings and phenomena show that the dynamics of coupled metronomes is very rich and may also serve as paradigm of synchronization and complex dynamics.

I. INTRODUCTION

Synchronization is a common phenomenon in nature and in our daily technical environment as well.[1,2] The first scientific approach to describe it can be dated back to 1665 when Christian Huygens discovered antiphase synchronization of two pendulum clocks, which were fixed at the same wooden beam.[3] In nature a spectacular example is given by the simultaneous flashing of fireflies at riverbanks in Southeast Asia.[4] Synchronization also turned out to be of functional importance in physiology and life sciences, where, for example, circadian rhythms adjust to external driving.[1] Another example are epochs of synchronization between fetal and maternal heart rate that can be influenced by maternal respiration.[5] The study of synchronization is also of technical importance, as the example of the Millennium Bridge in London shows. At the opening of the bridge on June 10, 2000, dangerous oscillations of the bridge occurred when pedestrians entered the bridge and it had to be closed again for safety reasons. Strogatz *et al.*[6] set up a model, which showed that if the number of pedestrians crossing the bridge (in its original design) exceeds a certain threshold, their footstep frequencies will synchronize and therefore lead to the observed oscillations of the bridge. This explanation is based on the so-called Kuramoto transition, a special kind of phase transition between a not synchronized and a synchronized state of a set of coupled oscillators. In the case of the Millennium Bridge the control parameter is given by the number of pedestrians on the bridge. The framework of Kuramoto transitions provides indeed a very general concept to explain synchronization in sets of coupled oscillators. Since oscillations can be found in many physical systems, it is not surprising that the theory of Kuramoto transitions has a very wide range of applicability. To illustrate this, we would like to mention an example from the emerging field of spintronics. In a so-called spin transfer oscillator (STO), a spin polarized current drives the precession of a magnetic vortex. If several such STOs are placed close enough to each other they will synchronize.[7] The onset of the collective motion can be understood within the Kuramoto theory.

In this article we present numerical investigations of a globally coupled set of metronomes that are in some sense related to Huygens' clocks. Huygens' explanation for the synchronization made use of invisibly small stress waves, which mediate the phase locking by propagating through the clocks' shared wooden beam. The synchronization of the clicking metronomes can be easily perceived acoustically, and the coupling (mediated by a moving plate) can be observed directly. The acoustic perception of the metronome is so catchy, that metronomes can also be used as a driving force for synchronization, as should be obvious to any musician. In this context, Engbert *et al.*,[8] for example, studied

a)Electronic mail: hulrich@gwdg.de.

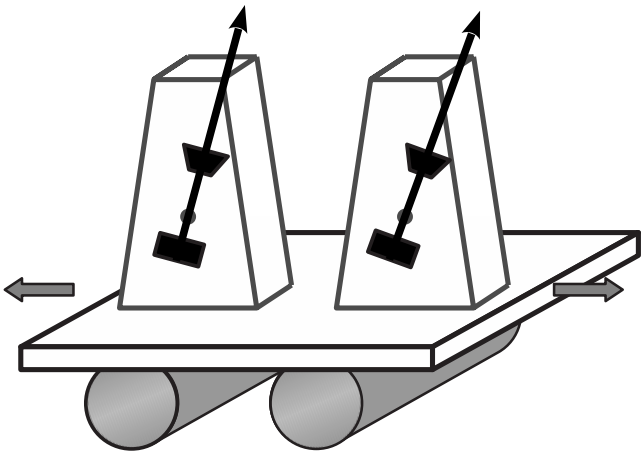

FIG. 1. Sketch of the simulated system for $N=2$ metronomes.

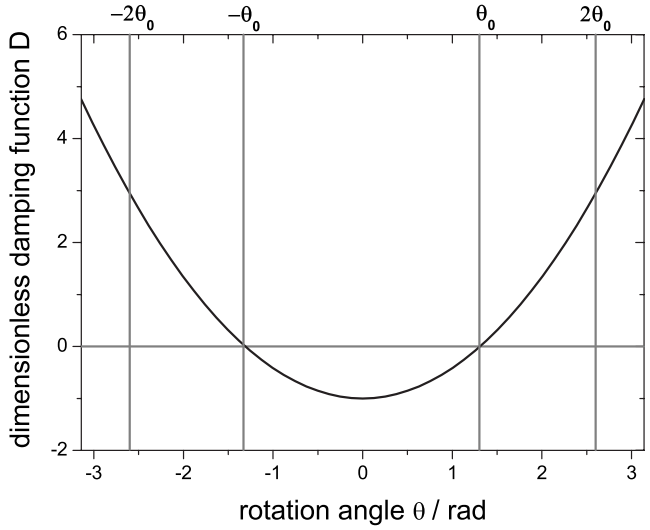

FIG. 2. The damping function $D(\Theta)$ for a $\Theta_0=75°$. The pendulum will be accelerated for $\Theta<\Theta_0$ and damped for larger angles. At $\Theta\approx 2\Theta_0$ the swinging pendulum comes to a rest, and then it starts swinging back. Note that for large Θ the damping diverges quadratically.

the synchronization of a human hand's movement with a metronome as a sound source.

The initial idea of our work comes from Pantaleone,[9] who combined investigations of real metronomes with analytical calculations. Extending Pantaleone's work, we present numerical simulations of a mathematical model for $N=2$, 3, and 100 metronomes and discuss their dynamical behavior.

II. FORMULATION OF THE PROBLEM

Pantaleone's original (experimental) setup consisted of two mechanical metronomes standing on a wooden plate. The plate was positioned on two empty soda cans, as illustrated in Fig. 1. Since the pendula's directions and the cans' axes are perpendicular, a bidirectional coupling between the metronomes is realized via the plate. The soda cans provide a support of small friction and due to their low masses (compared with the base plate and the metronomes) their angular momenta are small and will be neglected in the following.

This coupled system can be generalized to an arbitrary number N of metronomes of masses m_i and moments of inertia I_i. In this case, Pantaleone's equation of motion[9] reads

$$\frac{d^2\Theta_i}{dt^2}+\frac{m_i r_{cm,i} g}{I_i}\sin(\Theta_i)+\varepsilon_i\cdot D(\Theta_i)\cdot\frac{d\Theta_i}{dt}+\frac{m_i r_{cm,i}\cos(\Theta_i)}{I_i}\frac{d^2x}{dt^2}=0. \tag{1}$$

The term proportional to $\sin(\Theta_i)$ models the influence of the gravitational force. The eigenfrequency is given by $\omega_i=\sqrt{m_i r_{cm,i} g/I_i}$. Here $r_{cm,i}$ equals the distance of the metronome's center of mass to the pivot. To include the drive of the pendulum exerted by the metronome's escapement, Pantaleone[9] proposed a van der Pol term of the form $\varepsilon_i D(\Theta_i)d\Theta_i/dt$, where the damping function $D(\Theta_i)$ is given by

$$D(\Theta_i)=\left(\frac{\Theta_i}{\Theta_0}\right)^2-1. \tag{2}$$

This phenomenologically motivated function accelerates the pendulum if $\Theta_i<\Theta_0$ and damps the motion for $\Theta_i>\Theta_0$, generating the desired limit cycle: the metronome oscillates without external forces. In this way the motion of a single (uncoupled) metronome is for $\epsilon\ll 1$ roughly limited to $-2\Theta_0\le\Theta_i\le 2\Theta_0$.[9] Figure 2 illustrates the damping function. Since a realistic model requires for most metronomes a motion that is restricted to $\theta_i\in[-\pi,\pi]$, we choose θ_0 from the interval $(0,\pi/2)$. We will discuss the case of $\theta_0>\pi/2$ later on.

The last term of Eq. (1) accounts for the fact that the metronomes are inside a moving frame of reference. The motion of the plate generates a moment of inertia, which acts back on the metronomes. The time-dependent variable x describes the horizontal position of the plate. For the center of mass X all forces vanish. Therefore $d^2X/dt^2=0$.[9] For the plate's position x the following equation holds for the general case of N coupled metronomes:

$$x=-\sum_{i=1}^{N}\frac{m_i r_{cm,i}}{M+\Sigma_{j=1}^{N}m_j}\sin(\Theta_i). \tag{3}$$

Since we assumed the mass of the soda cans to be small compared with m_i and M, we do not include them in this formula and also neglect their moment of inertia. Furthermore, as stated by Pantaleone,[9] our description does not require any additional external forces, and any frictional effects (e.g., between the cans and the plate) are modeled by or are small compared with the van der Pol term.

To keep the following discussion as simple as possible, we only consider metronomes with equal masses $m_i=m$ and equal moments of inertia $I_i=I$. Furthermore, we choose $\varepsilon_i=\varepsilon$. With the average eigenfrequency $\omega=(1/N)\Sigma_{i=1}^{N}\omega_i$ a dimensionless time $\tau=\omega t$ is defined. If we assume that the deviation of the eigenfrequencies ω_i from ω is small for every metronome we can write

$$\frac{\omega_i^2}{\omega^2}=\left(\frac{\omega+\Delta\omega_i}{\omega}\right)^2=\left(1+\frac{\Delta\omega_i}{\omega}\right)^2\approx 1+2\frac{\Delta\omega_i}{\omega}=1+\Delta_i. \tag{4}$$

We will refer to Δ as the detuning of the metronomes. The motion of the base plate x is given by

$$x = -\frac{mr_{cm}}{M+Nm}\sum_{i=1}^{N}\sin(\Theta_i). \tag{5}$$

Here r_{cm} is meant in the sense of an average over all metronomes. This is a zeroth order approximation, which is justified because we assume only small deviations for ω_i from ω. In the case of real metronomes r_{cm} can usually be adjusted in order to change the eigenfrequency. Furthermore, we define a dimensionless coupling parameter $\tilde{\beta}$ according to

$$\tilde{\beta} = \frac{mr_{cm}}{M+Nm}\cdot\frac{mr_{cm}}{I}\cdot N. \tag{6}$$

In this equation the coupling parameter β from the original equation[9] is rescaled to a (total) coupling strength $\tilde{\beta}=\beta N$ in order to compare the results for different numbers of metronomes. With the definitions and considerations from above, the time evolution of the angle Θ_i can be expressed like this:

$$\frac{d^2\Theta_i}{d\tau^2} + (1+\Delta_i)\sin(\Theta_i) + \mu\cdot D(\Theta_i)\cdot\frac{d\Theta_i}{d\tau} - \frac{\tilde{\beta}}{N}\cos(\Theta_i)\frac{d^2}{d\tau^2}\sum_{i=1}^{N}\sin(\Theta_i) = 0. \tag{7}$$

For an arbitrary number N of metronomes, the system of Eq. (7) does not decouple. What remains is a differential algebraic equation (DAE) of the form $M\cdot\dot{\vec{x}}=f(\vec{x})$, where M is the so-called mass matrix. The DAE can be solved numerically. A definition of the mass matrix and the system of Eq. (7) as we have implemented them in MATLAB® (Ref. 10) is provided in the Appendix.

III. COUPLING OF TWO METRONOMES

We are now going to discuss the case of two coupled metronomes. The basic results of the simulations can be checked without too much effort using a real system of two metronomes.[9] While in the case of two metronomes Eq. (7) decouples and an approximate solution can be found analytically, our results are obtained using the solution of the DAE in the simplest case of $N=2$. As observed in the real experiment, the metronomes synchronize for a suitable set of the parameters $\tilde{\beta}$, Δ, and μ. After transient contributions fade out, the slightly different frequencies lock in to a common value and synchronization is stable for $t\to\infty$ within numerical accuracy. To illustrate the basic results we present in Fig. 3 a three-dimensional plot of the frequency difference f_1-f_2 of the metronomes as a function of the coupling strength $\tilde{\beta}$ and the detuning Δ. The frequencies were evaluated after transients decayed. This plot reveals a so called Arnol'd tongue for 1:1 synchronization. Any section parallel to the Δ-axis shows the typical plateaus in the $(f_1-f_2)-\tilde{\beta}$ plane. Note that in the case of two metronomes the eigenfrequencies are chosen such that $\Delta_1=+\Delta$ and $\Delta_2=-\Delta$ in Eq. (4).

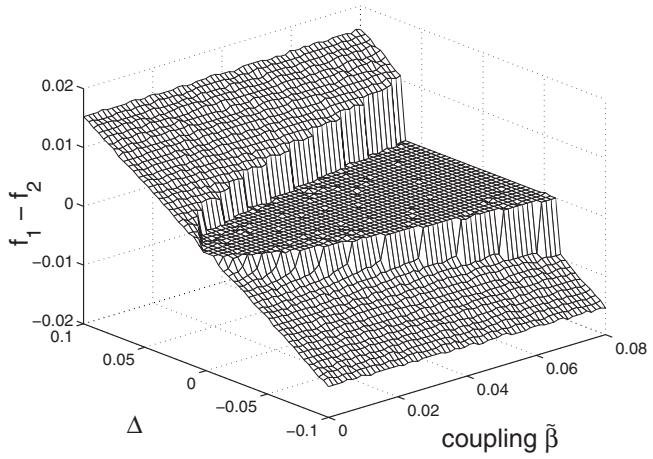

FIG. 3. Arnol'd tongue for 1:1 frequency synchronization. Plotted is the frequency difference f_1-f_2 vs the coupling strength $\tilde{\beta}$ and the detuning Δ. The tongue is visible as the flat area in the middle which is symmetric around $\Delta=0$. Note that Eq. (4) implies the relation between Δ and ω_i to be $\omega_i\approx\omega\sqrt{1+\Delta}$. The other parameters are $\mu=0.01$ and $\Theta_0=\pi/8$.

We should point out that the synchronization observed numerically is always in-phase, while antiphase synchronization appears not to be stable in the numerical solutions and is only found in transient processes. While this might again be due to inappropriate sets of parameters or initial values, it coincides with the observation that antiphase synchronization is hard to achieve in the real experiment, too.[9]

We now discuss the aforementioned case of increasing the van der Pol-angle Θ_0. For a value of $\Theta_0=\pi/4$ one observes a periodic oscillation of the metronome. If Θ_0 is larger than $\pi/2$, the metronome revolves. The gravitational force in Eq. (7) will then pull the pendulum down, corresponding to $\Theta=\pm 2\pi$. If we kept the damping function $D(\Theta)$ as introduced in Eq. (2), the damping would increase with $|\Theta|$ and thus stop the motion. However, we rather want the metronomes' angles Θ to be able to exceed values of $|\Theta|=\pi$ and then oscillate in the neighboring interval just like they do in the interval $(-\pi,\pi)$. Therefore, we modify our damping function $D(\Theta)$ to be 2π-periodic,

$$D(\Theta) = \left(\frac{\mathrm{mod}(\Theta+\pi,2\pi)-\pi}{\Theta_0}\right)^2 - 1. \tag{8}$$

This modified function is identical to the (original) function if $\Theta<\pi$ (see Fig. 4). For $\Theta>\pi$ it reproduces the original behavior of the metronome, which can now oscillate in the neighboring interval just as it did in the starting interval.

If we set Θ_0 slightly smaller than $\pi/2$, a metronome can only revolve if it receives a strong enough push from another metronome in the right moment. Approaching values of about $\pi/2$, there are two prominent values of Θ_0: passing the first one the metronomes are able to revolve, depending on the starting values, and do so individually. The metronomes will however stop after several overturnings and might change the direction of their rotation or stop overturning for some time. The projection of this chaotically rotating movement onto the Θ_1-Θ_2 plane can be labeled diffusive. We will discuss this behavior more thoroughly for the case of three metronomes. Increasing Θ_0 even further one passes the sec-

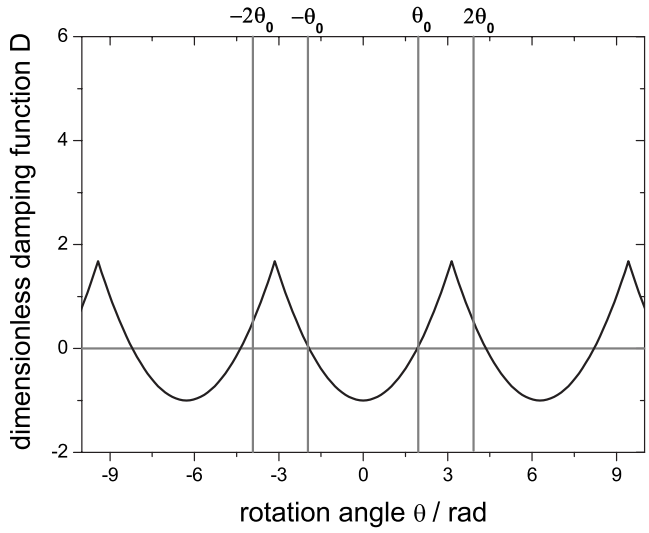

FIG. 4. Modified damping function $D(\Theta)$ for revolving metronomes. In this case, $\Theta_0=110°$. Thus, $2\Theta_0$ clearly exceeds π and we expect the (uncoupled) metronome to revolve.

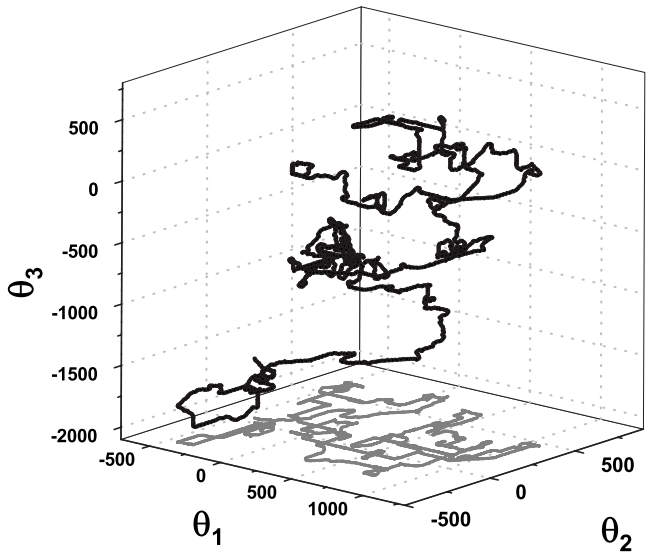

FIG. 6. Diffusionlike trajectory for three metronomes. The simulation parameters are $\tilde{\beta}=0.3$, $\Delta=0.015$, $\mu=0.01$, and $\Theta_0=\pi/2$. The eigenfrequencies were chosen equidistantly between $1-\Delta$ and $1+\Delta$.

ond critical value, after which the metronomes will monotonously overturn. In this case the system is in a state where continuous rotation is stable. Figure 5 illustrates the three cases, showing the angles Θ_1 and Θ_2 of the metronomes (which are defined to be unbounded for illustration purposes) as a function of time. Note that the realization of the third case shown in Fig. 5 is stable because both metronomes overturn in the same direction. If the two metronomes start overturning in different directions, one of them may change its direction at a certain point, after which the state of overturning becomes stable. This is in analogy to anti- and in-phase synchronizations.

IV. COUPLING OF THREE METRONOMES: PHASE DIFFUSION

Consider now the case that Θ_0 is just below $\pi/2$ so that the three metronomes may overturn due to the mutual coupling. How is this going to affect their dynamics? The second important parameter is again the coupling strength $\tilde{\beta}$. If we look at the Θ_1-Θ_2-Θ_3-space (which we will refer to as configuration space), as shown in Fig. 6, the overturnings create a kind of random walk—reminding the viewer of a diffusion controlled process. This chaotic movement is a kind of mixture between sections of monotonous overturnings and periodic oscillations. The monotonous sections are visible as parts of the trajectory where movement is in the simplest case (only one metronome overturns) parallel to one of the axes. The periodic parts of the trajectory form clews in the configuration space. These clews correspond to short metastable states when the motion is trapped in a cubic volume of the configuration space with an edge length of 2π. The different behaviors in these sections were already discussed for two metronomes.

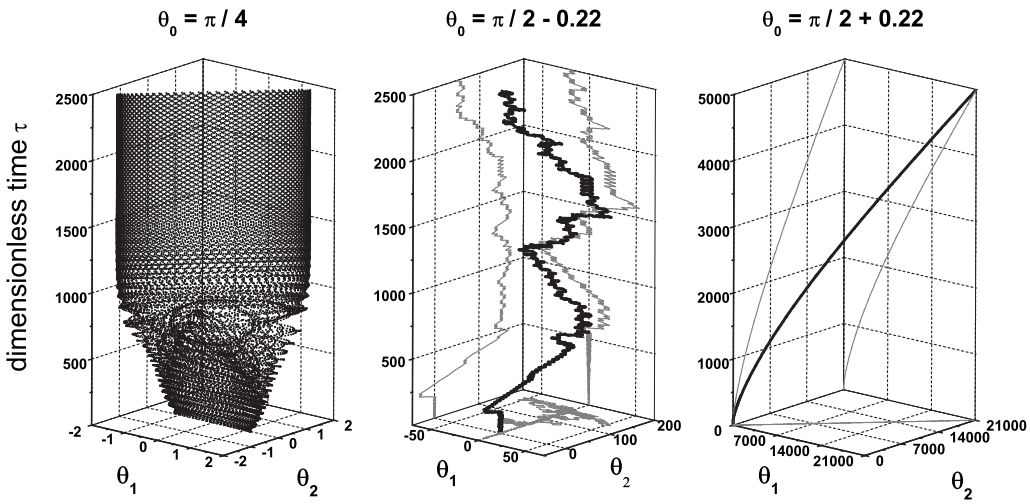

FIG. 5. Dynamics of two coupled metronomes for varying van der Pol-angle Θ_0 ($\tilde{\beta}=0.02$, $\mu=0.01$). From left to right the trajectories are periodically oscillating, chaotically rotating, and monotonously rotating.

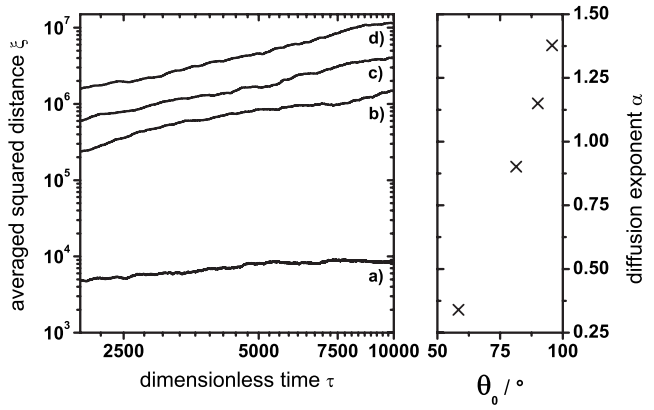

FIG. 7. Determination of the diffusion constant. The averaged squared phase distance was computed using 60 time series with different initial conditions for each value of the van der Pol angle: (a) $\Theta_0=58.4°$, (b) $\Theta_0=81.4°$, (c) $\Theta_0=90°$, and (d) $\Theta_0=95.7°$. In the left panel $\log \xi$ is plotted vs $\log \tau$ illustrating the occurrence of diffusive movement that obeys Eq. (9). The slope of the resulting (almost) straight lines can be used to estimate the diffusion exponent α. The right panel shows the diffusion exponent α as a function of Θ_0. All system parameters are the same as in Fig. 6.

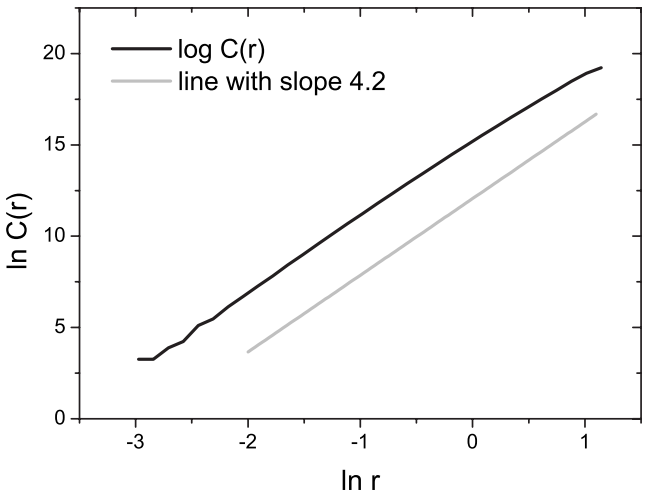

FIG. 8. Determination of the correlation dimension D_C of the diffusive dynamics shown in Fig. 6. The underlying trajectory has a total length of 2×10^5 points, covering a time which is twice as long as for the trajectory in Fig. 6.

In the case of generalized diffusion the averaged squared phase distance ξ obeys the equation

$$\xi := \left\langle \sum_i \Theta_i^2 \right\rangle = D\tau^\alpha, \tag{9}$$

where $\langle\cdot\rangle$ denotes an ensemble average (in our case computed for a number of different initial values). For $\alpha=1$ the diffusion is called normal, whereas for $\alpha<1$ the process is called subdiffusive and for $\alpha>1$ superdiffusive. Figure 7 shows that the larger the van der Pol angle Θ_0 is chosen, the more overturnings occur, and the higher are the diffusion constant D and the diffusion exponent α. Thus one can tune the behavior from sub- to superdiffusive.

For too small Θ_0 the revolving of the metronomes is just a transient phenomenon. On the other hand for too large van der Pol angles the metronomes are accelerated over a greater section of the $[-\pi,\pi]$-interval for Θ_i than damped. This favors continuously accelerated overturning of the metronomes because the van der Pol term in Eq. (7) effectively raises the total energy of the system in each cycle. However, in this case the coupling of the metronomes counteracts their constant rotation as long as they are not synchronized. Therefore, this regime begins only for $\Theta_0 \gg \pi/2$.

In order to quantify the seemingly chaotic behavior of the system, as shown in Fig. 6, we estimated the correlation dimension[11] D_C of the corresponding strange attractor. To obtain D_C we compute the correlation sum

$$C(r) = \frac{2}{N(N-1)} \sum_{k=1}^{N} \sum_{l>k}^{N} H(r - \|\vec{x}_k - \vec{x}_l\|) \tag{10}$$

using the $\sin(\Theta_i)$ and the angles' time derivatives $\dot{\Theta}_i$ at times $t_k=k\Delta t$ ($\Delta t=0.1$), which form the six-dimensional state vectors $\vec{x}_k$. H denotes the Heaviside function. Note that we have to use $\sin(\Theta_i)$ instead of Θ_i in order to compute $C(r)$ because the unbounded values of the Θ_i are not suitable for computing the correlation sum.

The correlation dimension

$$D_C = \lim_{r\to 0} \frac{\ln C(r)}{\ln r} \tag{11}$$

can be determined by the slope of the curve in Fig. 8. The estimated correlation dimension of $D_C=4.2$ supports the conjecture that we have a chaotic attractor.

V. COUPLING OF *N* METRONOMES: KURAMOTO TRANSITION

For a large number N of metronomes a Kuramoto transition is expected,[9] i.e., the synchronization of the pendula occurs abruptly if the coupling strength $\tilde{\beta}$ exceeds a certain threshold value. Figure 9 shows a plot of the Kuramoto parameter $R=|\Sigma_j \exp\{\imath\phi_j\}|$ as a function of $\tilde{\beta}$. The angle ϕ_j is defined as the phase space angle of the metronome j in the subspace of its variables θ_j and $\dot{\theta}_j$, which means $\phi_j=\arctan\{\dot{\Theta}_j/\Theta_j\}$. For the case of N metronomes the values for the detunings Δ_j are chosen from a Gaussian distribution with standard deviation Δ.

For every data point in Fig. 9 we integrated Eq. (7) long enough until transients decayed. For the upper curve, each point was calculated using the same initial conditions. For the lower curve, the initial conditions for each point were chosen randomly. Therefore the data scatter a bit more for the latter than for the upper curve, whose oscillating behavior for $\tilde{\beta}>0.03$ might be attributed to an intermittent, less synchronized state whose occurrence depends on $\tilde{\beta}$. In both cases one can determine a critical coupling strength of $\tilde{\beta}_{\text{crit}}\approx 0.01$ at which synchronization sets in.

To what extent does this critical coupling strength depend on the number N of metronomes? To examine this we will briefly compare the case of 100 with the case of two metronomes. In a Gaussian distribution with standard deviation σ (in our case $\sigma=0.05\equiv\Delta$) the average frequency deviation from the mean frequency is approximately given by

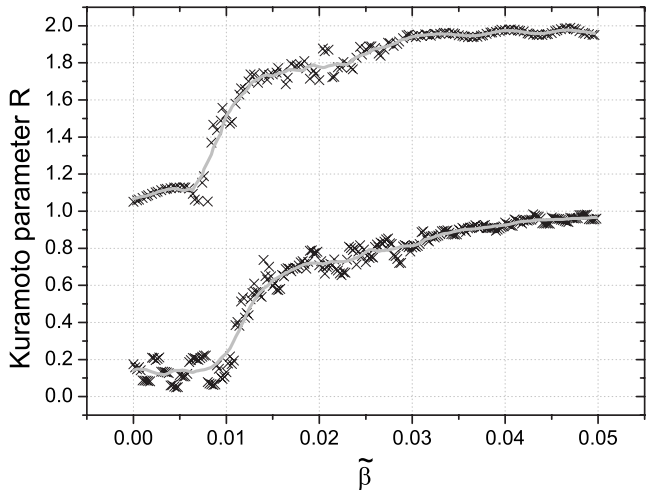

FIG. 9. Kuramoto transition for $N=100$ metronomes. The Kuramoto order parameter $R=|\Sigma_j \exp\{\imath\phi_j\}|$ vs the coupling strength $\tilde{\beta}$ shows a strong increase at about $\tilde{\beta}_{\text{crit}} \approx 0.01$. The upper and lower curves are obtained with fixed and random initial conditions, respectively, and the upper curve is shifted by one for better visibility. The experimental parameters were set to $\Delta=0.05$, $\mu=0.01$, and $\Theta_0=\pi/8$, thus avoiding overturnings. In both simulations the same set of eigenfrequencies ω_j was used.

$\sigma 0.4$. Therefore in our example for $N=100$ metronomes this deviation is given by $\Delta 0.4=0.02$. For the Arnol'd tongue shown in Fig. 3 we also simulated a "set" of two metronomes with nearly the same deviation $\Delta_j=\pm\Delta=\pm 0.025$. Comparing Figs. 3 and 9 one can easily see that for such a value of Δ_j synchronization sets in for roughly the same total coupling strength $\tilde{\beta}$ of about 0.01. We therefore conclude that the derived $\tilde{\beta}_{\text{crit}}$ is only marginally dependent on N.

VI. CONCLUSION

Our studies show that the general behavior of two or more bidirectionally coupled metronomes can be simulated numerically using equations of motion (7) with a van der Pol-like driving term. For the case of two metronomes the calculations yield the canonical results for in-phase synchronization, as shown by the example of the Arnol'd tongue in Fig. 3. Antiphase synchronization was not observed, which is in agreement with observations at real systems of metronomes. Extending the model to the situation where the metronomes are able to revolve the dynamics become more diverse. Varying the van der Pol-angle Θ_0 systematically opens up new regimes of the dynamics including chaotic diffusion.

For the case of three metronomes we could show that the type of diffusion can be changed from sub- to superdiffusive by the choice of Θ_0. For a large number of (nonrevolving) metronomes a Kuramoto transition is observed. It is noteworthy that the critical coupling strength $\tilde{\beta}_{\text{crit}}$ for 100 metronomes appears to be almost the same as for only two metronomes.

APPENDIX: NUMERICAL SOLUTION OF COUPLED PENDULUM EQUATIONS

In this appendix we briefly illustrate how we obtained our numerical solution by implementing the DAE in MATLAB®. Consider a system of N metronomes whose dynamics follows Eq. (7). The problem can be transformed into the form

$$M \cdot \vec{x} = f(\vec{x}), \tag{A1}$$

where $\vec{x}$ is a $2N$-dimensional vector comprising the phase angles and their derivatives,

$$\vec{x} := (\Theta_1, \dot{\Theta}_1, \ldots, \Theta_N, \dot{\Theta}_N)^t. \tag{A2}$$

The elements of the sparse $2N \times 2N$-matrix M are defined as follows:

$$\begin{aligned} j \neq k: & M_{2j,2k} = -\frac{\tilde{\beta}}{N}\cos(x_{2j-1})\cos(x_{2j-1}), \\ j = k: & M_{2j,2j} = M_{2j-1,2j-1} = 1. \end{aligned} \tag{A3}$$

In this definition $j,k=1\ldots N$. All other elements of M are zero. Finally, $f(\vec{x})$ can be written like this $(i=1\ldots N)$:

$$\begin{aligned} f_{2i-1} &= x_{2i}, \\ f_{2i} &= -(1+\Delta_i)\sin(x_{2i-1}) \\ &\quad - \mu\left[\left(\frac{\text{mod}(x_{2i-1}+\pi, 2\pi)-\pi}{\Theta_0}\right)^2 - 1\right] x_{2i} \\ &\quad - \frac{\tilde{\beta}}{N}\cos(x_{2i-1}) \sum_j^{1\ldots N} x_{2j}^2 \sin(x_{2j-1}). \end{aligned} \tag{A4}$$

One should keep in mind that an unsuitable set of parameters $\tilde{\beta}$, μ, and Δ easily leads to convergence problems. Especially a high value of the coupling parameter $\tilde{\beta}$ requires a very accurate calculation. Since synchronization as usual sets in at weak coupling ($\tilde{\beta}<0.02$ for $\mu=0.01$ and $\Delta \approx 0.01$) this does not pose a problem. For too large Δ_j Eq. (5) is a bad approximation. To avoid this one should then rather implement individual coupling strength $\tilde{\beta}_j$ for each metronome.

[1] A. Pikovsky, M. Rosenblum, and J. Kurths, *Synchronization-A Universal Concept in Nonlinear Sciences* (Cambridge University Press, Cambridge, 2001).
[2] S. Boccaletti, J. Kurths, G. Osipov, D. L. Valladares, and C. S. Zhou, Phys. Rep. **366**, 1 (2002).
[3] M. Bennett, M. F. Schatz, H. Rockwood, and K. Wiesenfeld, Proc. R. Soc. London, Ser. A **458**, 562 (2002).
[4] J. Buck, Q. Rev. Biol. **13**, 301 (1938).
[5] P. Van Leeuwen, D. Geue, M. Thiel, D. Cysarz, S. Lange, M. C. Romano, N. Wessel, J. Kurths, and D. H. Grönemeyer, Proc. Natl. Acad. Sci. U.S.A. **106**, 13661 (2009).
[6] S. H. Strogatz, D. M. Abrams, A. McRobie, B. Eckhardt, and E. Ott, Nature (London) **438**, 43 (2005).
[7] B. Georges, J. Grollier, V. Cros, and A. Fert, Appl. Phys. Lett. **92**, 232504 (2008).
[8] R. Engbert, R. Th. Krampe, J. Kurths, and R. Kliegl, Brain Cogn **48**, 107 (2002).
[9] J. Pantaleone, Am. J. Phys. **70**, 992 (2002).
[10] MATLAB® routines for solving the metronome differential algebraic equations can be downloaded from http://www.dpi.physik.uni-goettingen.de/software.
[11] P. Grassberger, Physica D **9**, 189 (1983).